BELL LABS INNOVATIONS

STRATEGIC WHITE PAPER

ELECTRICALLY SMALL ANTENNA ELEMENTS USING NEGATIVE PERMITTIVITY RESONATORS

Howard R. Stuart
Member, IEEE

Alex Pidwerbetsky
Member, IEEE

***Abstract*—**We show how resonators composed of negative permittivity materials can form the basis of effective small antenna elements. A quasi-static analysis of the resonant properties of a sub-wavelength negative permittivity sphere predicts that such a resonator will have a Q-factor that is only 1.5 times the Chu limit, matching the performance of other known electrically small spherical antenna designs, such as the folded spherical helix and the spherical capped dipole. Finite element simulation is used to demonstrate an impedance-matched radiating structure formed by coupling the resonator (a half-sphere above a ground plane) to a 50 ohm coaxial transmission line, where the coupling is mediated by a small conducting stub extending partially into the half-sphere. The resulting antenna has a $ka < 0.5$, and its bandwidth and efficiency performance corresponds well to that predicted by the quasi-static analysis of the resonator.

***Index Terms*—**Antennas, electrically small antennas, metamaterials, plasma antennas, Q factor, resonators.

Manuscript received March 18, 2005; revised January 26, 2006.
The authors are with the Bell Laboratories, Lucent Technologies, Whippany, NJ 07981 USA.
Digital Object Identifier 10.1109/TAP.2006.875498

TABLE OF CONTENTS

I. INTRODUCTION

The study of electrically small radiofrequency (RF) antenna elements is of both practical and fundamental importance. From a practical standpoint, emerging applications such multi-input multi-output (MIMO) mobile communications systems and RF-tagging benefit from the ability to make antenna size smaller. Fundamentally, it is well understood that as the antenna size enters the regime $ka < 0.5$ (where k is the free space wave number and a is the radius of the smallest sphere enclosing the antenna), the ability of the antenna to radiate effectively is substantially reduced[1]. This fundamental limitation is most commonly described in terms of the quality factor, Q, of the antenna. In the absence of material or conductor loss, the Q of an antenna element is proportional to the ratio of the energy stored in the antenna to the rate at which the antenna emits radiation. Because the operating bandwidth of an antenna varies inversely with Q, it is desirable to achieve as low a Q as possible when designing a small antenna for a specific application. Small antenna elements are typically characterized by large values of Q. There exists a fundamental relationship between antenna size and Q, referred to here as the Chu limit[2], which specifies the minimum Q achievable for an antenna of size ka. Of all of the problems typically encountered when designing small antennas (narrow bandwidth, impedance matching to low radiation resistance, low efficiency), the ability to design antennas whose performance approaches the Chu limit is the most challenging to solve.

In this paper, we consider the use of materials with negative electric permittivity as a building block for constructing effective small antenna elements. Although such materials do not occur naturally at microwave frequencies, negative permittivity can be realized at microwave frequencies using plasmas of the appropriate charge density. The behavior of antennas in the presence of plasmas was studied extensively in the 1960s[3–5], and the utilization of plasmas as antenna elements has also been proposed and studied[6,7]. Our work is distinguished from these earlier studies in that we are specifically considering the problem of using negative permittivity to construct an electrically small antenna element, and we directly compare its bandwidth performance to the Chu limit. As an alternative to using plasmas to realize negative permittivity, it is also possible to produce structures exhibiting negative electric permittivity behavior using periodic arrangements of conductors[8–10]. These structures, referred to as ***structured dielectrics*** or ***meta-materials***, have been used to demonstrate a range of interesting electromagnetic behavior at microwave frequencies, including negative permittivity, negative permeability[11], and negative refractive index[12–14]. Studying the behavior of electrically small negative permittivity resonators and antennas can potentially lead to the development of new antenna designs based upon conventional materials.

In this paper, we present a theoretical analysis and numerical simulation where we assume the existence of a material whose electric permittivity obeys the Drude dispersion relationship with a plasma frequency in the microwave regime. We address the specific question as to whether such a material would be appropriate for constructing a high-performance electrically small antenna. The use of double negative materials (both negative permittivity ***and*** negative permeability) has been considered previously as a means of improving the power radiated by electrically small antennas[15–17]. Here we show that negative permittivity alone is sufficient for constructing an effective small antenna element, and we clarify the issue of the radiation Q of such an antenna. We show here that, in the case of a solid negative permittivity sphere, the Chu limit can be approached, but not exceeded. In contrast to the work in[15], which considered the effect of a double negative spherical shell on an elementary dipole radiator placed at the center of the sphere, we study the problem from the point of view of a practical antenna geometry, including an impedance-matched transmission line feed. Although the properties of the antenna we describe are determined through numerical simulation, we show that the Q-factor and efficiency are directly related to the properties of the isolated resonator, which is significant, as the properties of the negative permittivity spherical resonator are well understood from studies of metal nanoparticles at optical frequencies[18]. These properties can, in fact, be well-predicted by a simple quasi-static analysis of the sub-wavelength negative permittivity sphere. The quasi-static analysis provides an analytical expression for the Q-factor that fully accounts for the frequency dispersion of the electric permittivity. This is a critical point, as neglecting the frequency dispersion can lead to the incorrect conclusion that such structures have bandwidths exceeding the Chu limit.

In Section II, we use the quasi-static analysis to derive a set of analytical equations describing the resonant bandwidth and scattering efficiency of a sub-wavelength sphere of negative permittivity material. The results of this analysis predict that this structure is characterized by a resonance with a radiation Q-factor that is only 1.5 times the Chu limit. This is an excellent result, suggesting that such a structure would make an effective small antenna element. In Section III, we compare the properties of the negative permittivity sphere to two known electrically small spherical resonator designs, the folded spherical helix[19,20] and the spherical capped dipole. We show that the bandwidth performance of these three resonators is similar, a fact that can be attributed to the spherical geometry inherent to each design. This suggests that the excellent bandwidth performance of the negative permittivity sphere is not due specifically to the negative permittivity material. Rather, it is the geometry that we have chosen (a spherical resonator) that allows us to so closely approach the Chu limit. (This is consistent with the recent analysis by Tretyakov ***et al.***[21], which concludes that a complex material covering can improve the Q-factor of an antenna if the covering itself participates in the radiation process.) It is known from the work of Wheeler in the 1950s[22] that a properly constructed self-resonant sphere provides good small antenna bandwidth. The use of a negative permittivity material simply provides one possible approach for synthesizing a sub-wavelength self-resonant spherical object.

In Section IV, we demonstrate, through a finite element simulation, that a half-sphere of negative permittivity material placed next to a ground plane can be coupled to a 50 ohm coaxial transmission line in order to produce a small antenna whose Q matches that predicted by the quasi-static analysis of the isolated resonator. The coupling between the resonator and transmission line is mediated by a small conducting stub that extends partially into the half-sphere, and the length of this stub is adjusted in order to obtain a good impedance match. In Section V, we discuss the general issues encountered when designing small antennas based on negative permittivity, specifically addressing the effects of resonator size and material absorption. The design principals discussed here can be easily extended to other resonator shapes, other kinds of transmission line feeds, and potentially to materials with negative permeability or negative index of refraction. Finally, in Section VI we briefly discuss the issue of practical implementation of the ideas presented in this paper.

II. QUASI-STATIC ANALYSIS

We choose to study our proposed antenna geometry by first considering the electromagnetic properties of the resonator forming the antenna (the electrically small negative permittivity sphere). We do this because the scattering properties of such resonators are well understood, and can be analyzed using asimple quasi-static analysis. Although this analysis is approximate, in the size regime $ka < 0.5$ it is very highly accurate. The quasi-static approximation allows us to incorporate, directly into the analytical equations, the frequency dispersion of the negative permittivity material. This is critical to deriving a physically valid formula for the Q-factor of the resonance, as any material with negative permittivity must be dispersive in order not to violate causality. We present here the quasi-static solution for the solid sphere resonator with negative electric permittivity. This sort of analysis could also be applied to other resonator shapes (e.g., ellipsoids, spherical shells), as well as to resonators consisting of materials with negative permeability.

We begin by assuming the availability of a material with a frequency dependent permittivity $\varepsilon(\omega)$ specified by the following equation:

$$c(\omega) = 1 - \frac{\omega_p^2}{\omega(\omega + i\gamma)} \tag{1}$$

where ω_p is the plasma frequency and γ represents material absorption. Equation (1) is often referred to as the Drude dispersion relationship. Our motivation in these studies is to explore the ultimate performance achievable in our antenna designs and to establish a set of requirements for the creation of appropriate materials with which to form these structures. We therefore assume that ω_p can be specified as required, and we will study the performance under conditions of both zero and non-zero values of loss.

It is well-known from studies of metal at optical frequencies that materials with permittivities obeying (1) exhibit a wide range of interesting physical effects, including the presence of surface plasmons at flat boundaries[23], and localized plasmon resonances in sub-wavelength particles[18]. Very strong localized resonances occur, for example, in sub-wavelength spheres when $\omega = \omega_p/\sqrt{3}$ ($\varepsilon = -2$). The resonant modes associated with negative permittivity spheres are notably different in character than those associated with positive permittivity spheres. Although the properties of these resonances are well-known, we review them here for the benefit of the reader. Figure 1 shows the scattering cross-section of sub-wavelength spheres of various radii, with a permittivity obeying (1) with $\gamma = 0$, as calculated using Mie theory (the exact solution of the scattering of electromagnetic radiation by spheres)[18]. We see in Figure 1 that the scattering resonances exist regardless of how small we make the sphere, and that the resonant frequency approaches a value of $\omega = \omega_p/\sqrt{3}$ as the sphere becomes infinitesimally small. The shift in resonant frequency as the size of the sphere increases is actually a second-order effect associated with the breakdown of the electrostatic approximation for spheres with non-zero radii. The limiting resonant frequency for a sphere with radius $a \ll \gamma$ can be deduced simply by examining the well-known equation for the electrostatic polarizability of a sphere[24]

$$\alpha = 4\pi a^3(c-1)/(c+2) \tag{2}$$

where the total dipole moment $\vec{P}$ (the volume integral of the polarization within the sphere) is defined according to equation $\vec{P} = \varepsilon_o a \vec{E}$ (ε_o is the permittivity of free space and $\vec{E}$ is the applied electric field) and f is the permittivity of the sphere. Here we see that when $\omega = \omega_p/\sqrt{3}$, the permittivity $f = -2$ and the polarizability is singular. Radiative damping, which is not accounted for in the electrostatic calculation, insures that the polarizability actually remains finite, as we show below. However, the electrostatic calculation accurately predicts the frequency of the resonance, and it also allows us to deduce the salient properties of the resonant mode. In electrostatics, the electric field induced inside a sphere by a uniform applied electric field is itself uniform. The uniformly polarized sphere induces a field outside the sphere that is equivalent to that due to a dipole placed at the center of the sphere[25]. Mie theory confirms that the fundamental resonant mode of

Figure 1 | Recursive Estimation Solution Model

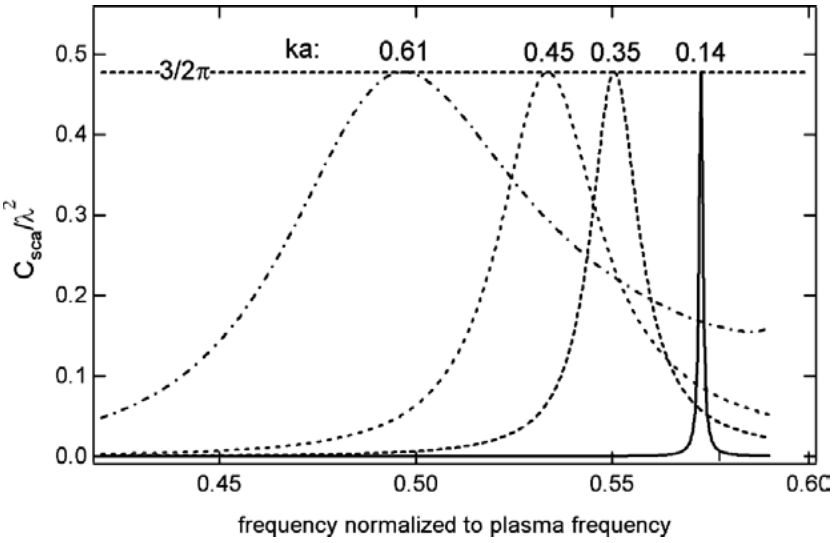

Figure. 1. Scattering cross-section versus frequency for spheres of varying radii with electric permittivity obeying the Drude dispersion relationship. The scattering cross-section is normalized to the square of the resonant wavelength for each curve. In the absence of loss, the resonant cross-section remains constant for vanishingly small radii, whereas the width of the resonance becomes much narrower (in concordance with the Chu limit). The resonant frequency asympotically approaches $\omega_p/\sqrt{3}$ for small radii, as predicted by electrostatics.

the negative permittivity sphere is characterized by a uniform polarization within the sphere, and that it radiates as an electric dipole (the lowest order spherical harmonic, or TM_{10} mode)[18]. The dipolar nature of the resonant mode is confirmed in Figure 1 by noting that the peak scattering cross-section of each of the resonators (regardless of size) achieves a value of $3\gamma^2/2\pi$ as is characteristic of a dipole radiator[26].

The properties of the negative permittivity sphere differ dramatically from that of a positive permittivity sphere in many respects. In spheres of purely positive electric permittivity, particles that are much smaller than the wavelength will not scatter incident radiation very effectively, as the resonances of these spheres appear only once the sphere exceeds a certain minimum radius ($k_d a = 3.05$ for the fundamental TE mode, where $k_d = \sqrt{\varepsilon} k$ [27]). Thus, the fundamental resonant frequency varies inversely with the radius of the sphere, unlike the case of the negative permittivity sphere, where it is predominantly size independent. Furthermore, the fundamental resonant mode of the positive permittivity sphere is not uniformly polarized within the sphere, but rather contains a null in the electric field along the central axis of the sphere. It is important to recognize, therefore, that knowledge and intuition derived from the case of the positive permittivity sphere cannot be applied towards understanding the behavior of the negative permittivity sphere.

When considering the scattering behavior of the negative permittivity sphere shown in Figure 1, we see that as the particle size is made smaller, the width of the resonance becomes much narrower. This is consistent with what is predicted by the Chu limit. According to Chu[2], the Q of an antenna (or equivalently, the Q of any self-resonant object with a single electric or magnetic dipole resonance) must obey the relationship $Q \geq 1/(ka)^3 + 1/ka$ [28]. Therefore, decreasing the size of the resonator increases its Q and narrows its bandwidth. It is our goal in this paper tounderstand the applicability of negative permittivity structures to the problem of electrically small antennas. The relevant question to pose here is how close the negative permittivity sphere comes to matching the fundamental limits on Q. In order to do this, we must evaluate the Q of

the negative permittivity sphere. This can be deduced exactly from Mie theory, using the numerical data from the curves in Figure 1, with the Q being equal to the inverse of the normalized 3 dB scattering bandwidth. However, for spheres with $ka \ll 1$, a quasi-static approach can be employed to determine an analytical equation for Q that is highly accurate when compared to Mie theory. This approach was originally used to study the resonant electric field enhancements in metal nanoparticles for surface enhanced Raman scattering applications[29], and we extend this approach here for the determination of the radiation Q of the small negative permittivity sphere.

We begin with (2), the electrostatic polarizability of the sphere. In order to determine the Q of the resonance, we must include the effects of radiative damping. We do this by noting that the total induced polarization $\vec{P}$ will introduce a radiation reaction field $\vec{E_r} = i(2/3)k^3\vec{P}/4\pi\varepsilon_o$ [24], due to the fact that the resonant mode of the sphere radiates as a pure electric dipole. This enables us to write the polarization of the sphere as

$$\vec{P} = \alpha\varepsilon_o\left[\vec{E} + i\frac{2}{3}\frac{k^3}{4\pi\varepsilon_o}\vec{P}\right]. \tag{3}$$

In (3), we see that $\vec{P}$ now appears on both sides of the equation. If we solve (3) for $\vec{P}$, we can define an effective polarization α_{eff} to be

$$\alpha_{\text{eff}} = \frac{\alpha}{1 - i\frac{\alpha}{1\pi}\frac{2k^3}{3}}. \tag{4}$$

As a check, we can evaluate (4) when $\varepsilon = -2$, and we see that the resonant scattering cross-section (defined as $C_{\text{sca}} = (k^4/6\pi|\alpha_{eff}|^2)$ [18] reduces to $C_{\text{sca}} = (3/2\pi)\lambda^2$, consistent with the results predicted by Mie theory in Figure 1, and expected for a resonant mode radiating exclusively into the TM_{10} mode.

By combining (4) and (2) we can express the scattering cross-section of the sub-wavelength sphere as

$$C_{\text{sca}} = \frac{8\pi}{3}k^4a^6\frac{(\varepsilon-1)^2}{(\varepsilon+2)^2 + (\varepsilon-1)^2\left(\frac{2k^3a^3}{3}\right)^2}. \tag{5}$$

By combining (5) and (1) and assuming for the moment that $\lambda = 0$ (no loss), we can derive the complete quasi-static expression for the scattering cross-section as a function of frequency for the negative permittivity sphere

$$C_{\text{sca}} = \frac{8\pi}{3}k^4a^6\frac{\omega_o^4}{\left[(\omega-\omega_o)(\omega+\omega_o)\right]^2 + \left[\omega_o^2\frac{2k^3a^3}{3}\right]^2} \tag{6}$$

where $\omega = \omega_p/\sqrt{3}$ is the resonant frequency of the sphere. Around the resonant frequency, $\omega = \omega_o \approx 2\omega_o$, and (6) can be simplified to the following form:

$$C_{\text{sca}} = \frac{2\pi}{3}k^4a^6\frac{\omega_o^2}{(\omega-\omega_o)^2 + \left(\omega_o\frac{k^3a^3}{3}\right)^2}. \tag{7}$$

Equation (7) is immediately recognizable as a Lorentzian. Note that in Figure 1, the variation in frequency as the particle size increases is due to retardation effects that are not accounted for by the quasi-static analysis; however, (7) does provide

exact predictions of the peak scattering cross-section and Q when compared with the results of Mie theory in the limit of small spheres ($ka \ll 1$). We deduce the analytical formula for the Q-factor of the resonance from the second term in the denominator of (7), which for the Lorentzian can be expressed in terms of the Q as $[\omega_o/(2Q)]^2$. This yields the following formula for the Q of the negative permittivity spherical resonator:

$$Q = \frac{3/2}{(ka)^3}. \tag{8}$$

In the regime $ka \ll 1$, the Q of the negative permittivity resonator is exactly 1.5 times the Chu limit. Although the properties of spherical negative permittivity resonators are well understood, it is not widely appreciated that the of such resonators approaches the Chu limit so closely. We can assess the accuracy of (8) by comparing it to the 3 dB scattering bandwidths predicted by Mie theory (Figure 1). In the limit $ka \ll 1$, the correspondence is nearly exact; for the case of a sphere with $ka = .045$, (8) predicts the Q with an accuracy of 2.3% compared with Mie theory. Thus, the quasi-static analysis can be applied accurately over all values in the small antenna regime ($ka < .05$. (We note here that $k = 2\pi/\lambda$ is always taken to be the free-space value in our analysis.) Equation (8) is indeed an excellent result, as it suggests that negative permittivity resonators would make effective small antenna elements.

It is important to take into account the effects of material absorption on the radiative efficiency of the resonators used to form a small antenna element. All results presented above on the Q of the resonators assumed that the loss parameter $\lambda=0$. If we now include non-zero loss values, we can evaluate the scattering efficiency of the sub-wavelength sphere using the expression

$$\text{eff} = \frac{C_{\text{sca}}}{C_{\text{sca}} + C_{\text{abs}}} \tag{9}$$

where C_{sca} and C_{abs} are the scattering and absorption cross-sections respectively. The denominator of (9) represents the total loss cross-section (absorption plus scattering), and is determined from the equation $C_{sca} + C_{abs} = k\text{Im}[\alpha_{\text{eff}}]$.[18] Combining (9), (4), and (2), and expressing the permittivity as $\varepsilon = \varepsilon_r + i\varepsilon_i$, we arrive at the following result for the scattering efficiency of the sub-wavelength sphere (the algebraic steps of the derivation are omitted for brevity)

$$\eta = \frac{1}{1 + \frac{\varepsilon_i}{2(ka)^3}}. \tag{10}$$

Figure 2 shows a contour map of efficiency as a function of the imaginary component of the permittivity ε_i and the size ka of the antenna. For a given value of ε_i there is a direct tradeoff between scattering efficiency and size (larger spheres will have larger scattering efficiencies) [30]. In order to achieve a scattering efficiency greater than 50%, we must satisfy the criteria $\varepsilon_i < 2(ka)^3$. For a sphere with $\alpha = \lambda/10$, we must have $\varepsilon_i < 0.5$, and for $\alpha = \lambda/20$, the criteria becomes $\varepsilon_i < 0.06$. This result suggests that material loss (in addition to required bandwidth) will determine the ultimate limit on the smallest achievable size of an antenna based upon localized plasmon resonances.

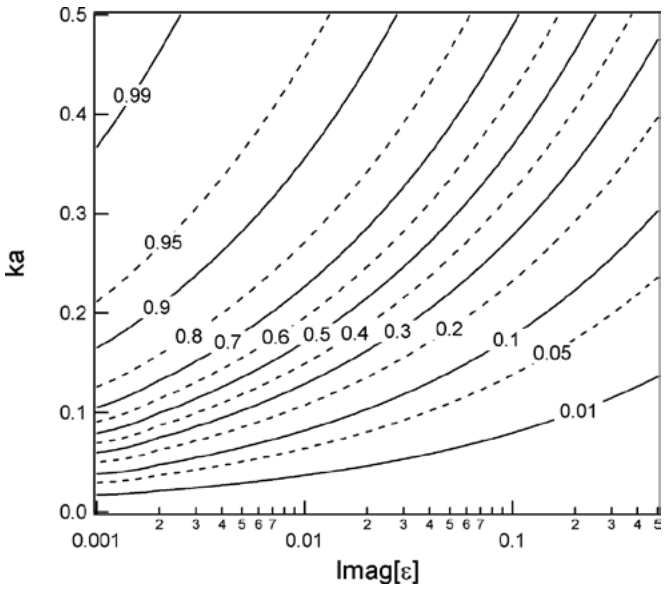

FIGURE 2

Contour plot of scattering efficiency versus the size parameter ka and the loss parameter ε_i (the imaginary part of the permittivity), for a sub-wave-length sphere obeying the Drude dispersion relationship. For a given value of ε_i, there exists a clear tradeoff between size and efficiency.

III. COMPARISON TO KNOWN SPHERICAL RESONATOR DESIGNS

In order to put the negative permittivity sphere into some perspective, we compare its properties to two examples of known resonator designs whose bandwidth performance does come close to the Chu limit. The two resonators considered here are the folded spherical helix [Figure 3(a)],[19,20] and the spherical capped dipole [Figure 3(b)]. Each of these resonators can be designed to be electrically small ($ka < .05$ at the resonant frequency), and each has a Q-factor that can be made close to ~ 1.5× the Chu limit (the exact value depends upon the particular design parameters of the resonator).

The folded spherical helix illustrated in Figure 3(a) consists of four identical nested helix arms at 90 degree spacing; each arm makes 1.25 turns in going from the pole to the equator, and then reverses direction. The direction reversal insures that the magnetic dipole component of the current cancels so that the resulting resonator has a lowest order resonance that is a pure electric dipole. Finite element simulation was used to determine the resonant frequency and Q-factor of this resonator: it has a normalized size $ka = .031$ and a Q-factor that is ~1.6 times the Chu limit. Recent work by Best[19,20] has shown how such resonators can be made into antennas with near Chu limit performance using a relatively simple feed geometry.

The spherical capped dipole shown in Figure 3(b) consists of a simple straight wire capped with hemispherical conductive shells. The resonant frequency depends strongly upon the size of the equatorial gap (which affects the capacitance of the structure). In the example shown in Figure 3(b), the gap size is 3/4 of the radius. This resonator has a normalized size $ka = .034$ at the resonant frequency, and a Q-factor that is ~1.5 times the Chu limit. For comparison, we illustrate the electric field profile of the resonant mode of these two resonators, along with that of the negative permittivity sphere, in Figure 4.

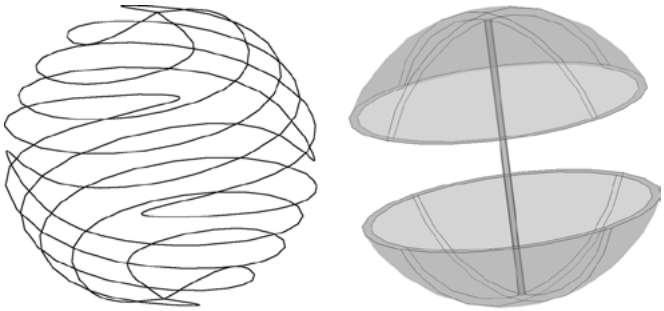

FIGURE 3

(a) Folded spherical helix resonator. (b) Spherical capped dipole resonator. Each of these resonators can be designed to be electrically small and have a Q-factor near 1.5 times the Chu limit.

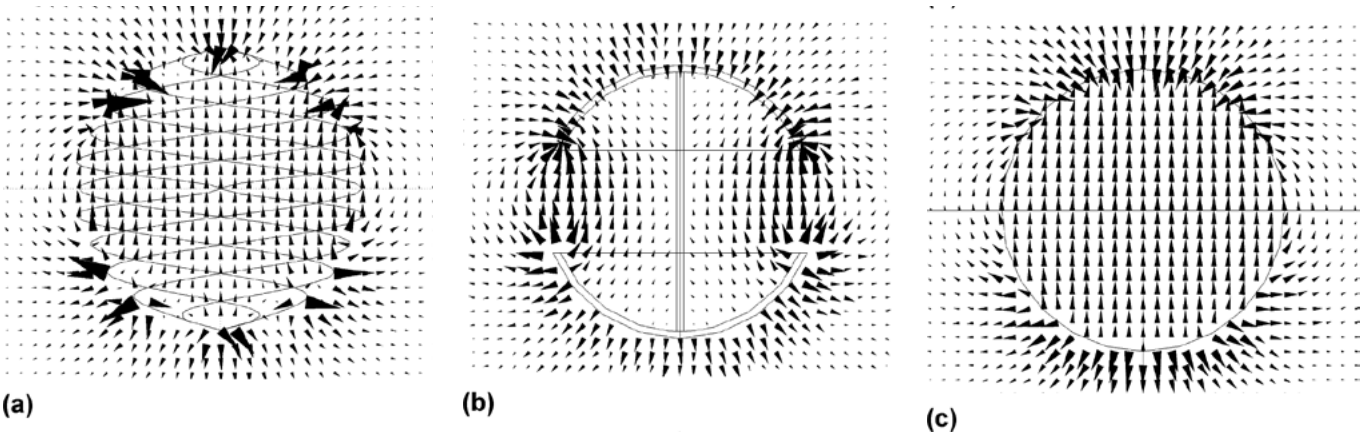

FIGURE 4

Electric field profiles of the resonant mode of (a) the folded spherical helix, (b) the spherical capped dipole, and (c)the negative permittivity sphere. The sign reversal of the electric field across the surface of the sphere at the poles in (c) is characteristic of the negative permittivity sphere, and can be attributed to theboundary conditions on the normal component of the displacement. It is interesting that similar behavior is observed in the mode of the spherical helix in (a), though there is nonegative permittivity material in this case.

The trait that these three resonators share is that they are all spherical. It is well-known from the work of Wheeler[22,31,32] that optimizing the bandwidth of an electrically small antenna requires making optimal use of the spherical volume occupied by the antenna. The resonances in the spherical helix and spherical capped dipole arise from the inductance and capacitance inherent to the structures; the main difference between the two is how the inductance and capacitance is distributed geometrically within the spherical volume. In the case of the folded spherical helix, the inductance is confined to surface of the sphere, whereas in the spherical capped dipole the inductance is concentrated along the central axis of the sphere. The negative permittivity resonator can be interpreted in a similar manner: it has an inductance that is distributed uniformly throughout the spherical volume. Engheta ***et al***.[33] have recently shown how it is possible to model negative permittivity spheres as inductor elements; the negative permittivity material effectively forms a spherical inductor, which then resonates with the fringe capacitance surrounding the sphere [33]. (In the context of plasmas, the resonance of the negative permittivity sphere is often explained as a localized resonant oscillation of conduction electrons.) The comparable bandwidths of the three resonators suggests that the good bandwidth performance of the negative permittivity sphere is not due specifically to the negative permittivity material itself, but rather to the geometry we have chosen (the sphere). The role of the negative permittivity material is to create the inductance necessary to establish the resonance within the electrically small structure.

The negative permittivity sphere provides bandwidth performance close to the Chu limit and matching that of known spherical resonator designs such as the folded spherical helix and the spherical capped dipole. Each of the latter two resonators can be made into antennas using an appropriate impedance-matched transmission line feed. In the next section, we present numerical simulations of an impedance-matched feed geometry that enables the negative permittivity sphere to form an antenna.

IV. HEMISPHERICAL ANTENNA ELEMENT

Using the quasi-static analysis, we have derived the properties of electrically small spherical resonators composed of negative permittivity materials. In order to form a complete antenna element, the resonator must be coupled to a transmission line. To verify the applicability of the quasi-static analysis presented in Section II to the performance of actual antenna elements, we consider an antenna of the geometry shown in Figure 5. In this geometry, a half sphere of negative permittivity material is placed on a ground plane, and fed through its center by a coaxial transmission line terminated with a small monopole stub. The geometry is such that the half sphere is perfectly centered about the coaxial line and the small stub extends partially into the negative permittivity material. This geometry is chosen for two reasons. The first is that the fundamental resonant mode of the negative permittivity sphere exhibits a uniform electric field within the sphere [see Figure 4(c)]; the small stub protruding into the center of the sphere thus provides a strong coupling between the coaxial transmission line mode and the resonant mode of the sphere. (This would not be the case for the positive permittivity sphere, which has a null in the electric field along its center axis in its fundamental mode.) The second reason is the rotational symmetry of the geometry allows the numerical simulations to be done in two-dimensions, reducing computational complexity. By using a half sphere above a ground plane, we are able to create an example where the electrical size of the antenna (*ka)* is precisely the size of the resonator. (We have neglected the size of the ground plane in our evaluation of *ka*; this is valid for a monopole over an infinite ground plane, where the equivalent dipole version of the antenna with no ground plane would have the identical value of *ka* [19,34].)

All simulations are done with the finite element method (using the commercial solver Femlab[35]) with a first order absorbing boundary condition implemented at a surface that is placed at one to three wavelengths from the antenna element. The coaxial transmission line has an inner conductor radius of 3 mm and an outer conductor radius of 7 mm, resulting in a nominally 50 ohm impedance. The radius of the sphere is chosen to be 8 mm and the length of the stub is varied in order to find the optimum impedance match. The negative permittivity material has a dispersion relationship obeying (1) with a plasma frequency of 3.54 GHz. In the numerical simulation, the two sharp corners occurring at the termination of the transmission line (stub tip and ground plane corner) were rounded to a 100 μm bend radius, and a small imaginary component ($\gamma = 2 \times 10^{-6}\omega_p$) was added to the permittivity of the sphere.

This improved numerical stability (results were checked at various increasing mesh densities to insure consistency) and resulted in only a very small efficiency penalty (efficiencies were >99.5%).

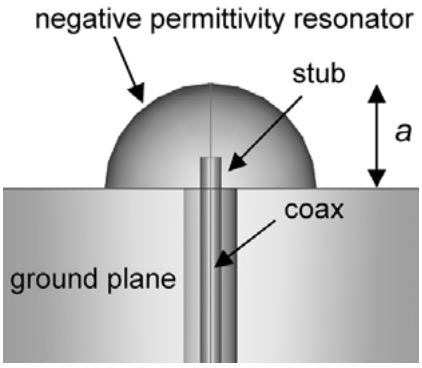

FIGURE 5

Antenna element based upon a half-sphere of material with negative permittivity placed at the termination of a coaxial transmission line. The radius of the sphere is 8mm, and the operating wavelength of the antenna is 148 mm, leading to *ka* = 0.34.The element is driven by a short conducting stub that extends from the coaxial line in to the material; the stub length is adjusted to obtain a good impedance match.

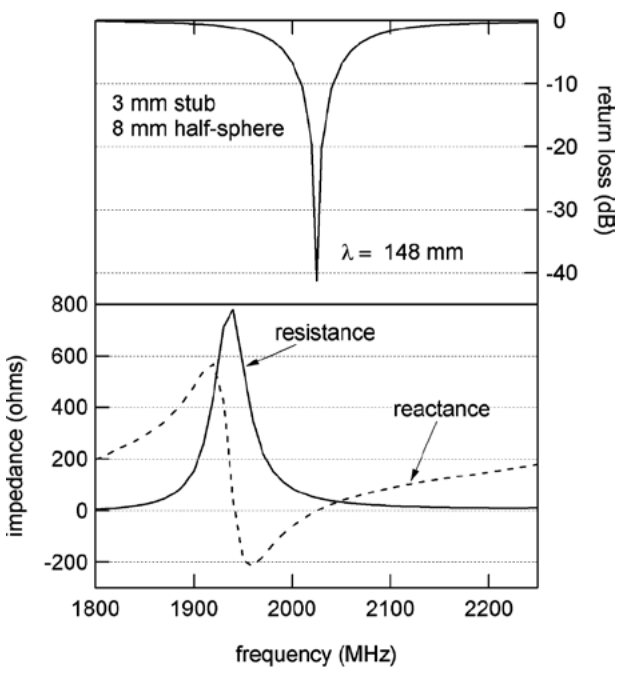

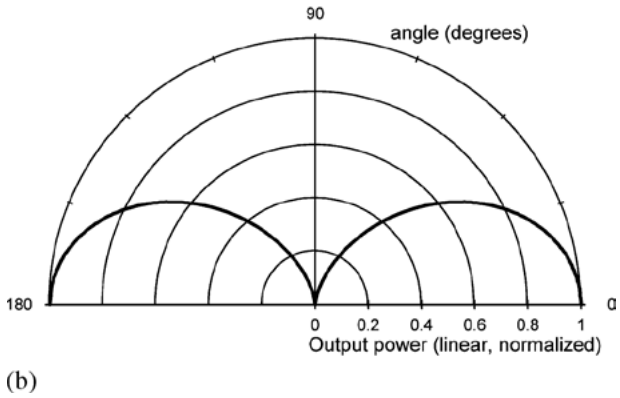

FIGURE 6

(a)Top: return loss versus frequency for the antenna pictured in Figure5 for a stub length of 3mm. Bottom: antenna impedance versus frequency. The plasma frequency of the half-sphere material is 3.54 GHz.
(b) Output radiation power of the antenna.

The optimum stub length was determined through simulation to be 3 mm, and the return loss and antenna impedance versus frequency for an antenna with this stub length are shown in Figure 6. One striking aspect of this antenna as compared to the conventional stub is its small size at the resonance frequency. At the antenna's resonant frequency of 2025 MHz (the frequency where the reactance is zero and the input impedance is matched to the transmission line), the operating wavelength is 148 mm, meaning that the 3 mm stub length is roughly $\lambda/50$, and the overall antenna size is characterized by $ka = 0.34$ (radius $= \lambda/18.5$). The impedance behavior of the antenna is notably different than that of a conventional monopole antenna. In particular, the fundamental resonance of the antenna occurs at a frequency somewhat higher than the peak in the radiation resistance, (rather than the opposite case as for the conventional monopole). At very low frequencies (not shown on the plot), the reactance remains positive, indicating that the termination is inductive at low frequency, rather than capacitive, as is the case for the conventional monopole. In these respects the antenna more closely resembles the folded spherical helix antenna[19] rather than the conventional monopole. This is not surprising, given the similarities between the negative permittivity resonator and the folded spherical helix resonator discussed in Section III. The negative permittivity sphere acts like an inductor, tuning out the capacitance inherent in the short monopole, and allowing the antenna to resonate at a very small size compared to the wavelength. (The use of a plasma as an inductor to tune out the capacitive reactance of a short antenna was demonstrated by Chen and Lin in 1968[5], but those authors made no attempt to compare the bandwidth of their antenna to fundamental limits). An alternative physical explanation for the small size of this antenna relates to the known properties of the negative permittivity spherical resonator. The resonant frequency of the antenna indeed corresponds closely to that of the fundamental mode of the negative permittivity sphere: this frequency occurs at roughly $0.57\omega_p$, very close to the value predicted by electrostatics for the sphere ($f = -2.06$), and slightly shifted from the value predicted by Mie theory (which is seen from Figure 1 to be $0.55\omega_p$ for a $ka = .035$ sphere). The antenna can therefore be viewed as a plasmon resonator that forms a resonant coupling between the transmission line mode and the

radiation mode. The output radiation pattern is shown in Figure 6(b), and confirms that the radiation mode of the antenna corresponds to that of a small vertical oscillating dipole, as expected for an antenna of this size.

The Q of the antenna can be estimated from the derivative of the antenna impedance Z at the resonant frequency using the following formula[36]:

$$Q \approx \frac{\omega_0}{2R_0} |Z'(\omega_0)| \tag{11}$$

where ω_0 is the resonant frequency and R_0 is the transmission line impedance at the resonant frequency. This formula yields a value of $Q = 42$ at the operating frequency of the antenna, a value which is ~1.47 times the Chu limit for an antenna with $ka = .034$ ($Q_{\text{Chu}} = 28.5$).

Thus, the quasi-static analysis presented in Section II is effective in predicting the actual bandwidth performance of the antenna element formed using this resonator. We note that (11) was derived in reference [36] and is generally valid in the regime where $Q > 4$. The Q estimated from (11) for our antenna not only corresponds to the Q predicted from the quasi-static theory, but also corresponds exactly to the 3 dB matched VSWR bandwidth observed in the return loss simulations (if one assumes that the normalized 3 dB matched VSWR bandwidth is $2/Q$, a relation that is also derived in [36]). We thus confirm that (11) appears to be valid for an antenna with negative permittivity, as was predicted in reference [36].

We can further test the predictions of the quasi-static theory by adding loss to the resonator material. Figure 7 shows return loss versus frequency simulations for the same antenna described in Figure 5, with the loss parameter $\lambda = 0.01 * \omega_p$. The performance of the antenna without loss is shown for comparison. When loss is added to the material, the resonant frequency does not change, but the response broadens slightly, and the depth of the return loss minimum is reduced to a –12 dB minimum. The performance can be improved by increasing the length of the stub; Figure 7 also shows the performance for a stub length of 4.5 mm. When the stub length is increased, the resonant frequency increases slightly and the return loss improves to nearly –30 dB on resonance (the reason for this will be discussed in the next section). The other impact of adding loss is, of course, a reduction in efficiency. Efficiency is plotted versus frequency in Figure 7 for the case of a 4.5 mm stub. Across the operating bandwidth, the efficiency is flat at a value of 61.4%; the quasi-static formula in (10) predicts an efficiency of 65.3% at the operating frequency of this antenna, indicating that the quasi-static analysis is able to predict the antenna efficiency with reasonable accuracy.

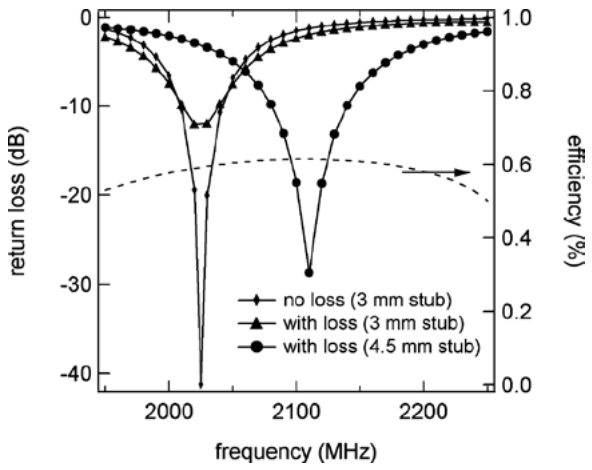

FIGURE 7

Return loss versus frequency for the antenna in Figure 5 including the effects of loss in the resonator material ($\lambda = 0.01 * \omega_p$), with a stub length of 3 mm (triangles) and 4.5 mm (circles). The optimized no-loss case is shown for comparison (diamonds). When loss is added to the material, the stub length must be increased to maintain an optimal impedance match on resonance, and the resonance frequency is then shifted to higher frequency.

V. DISCUSSION

The physical interpretation of the antenna as a resonant coupler between the transmission line mode and radiation mode can be used to understand the behavior of this antenna. This physical picture suggests a general formalism for designing electrically small antenna elements based upon negative permittivity materials. The first step is to design an appropriate resonator structure; here we have considered the case of a negative permittivity sphere, but we can also presume that other resonator shapes, as well as other resonator materials (for example, negative permeability, or negative refractive index materials) could also form the basis of the antenna design. The electrically small sphere is a particularly appealing case, because its behavior can be predicted by a simple set of analytical formulas, and because its bandwidth performance is especially close to the fundamental limits. The results presented here confirm that the properties of the isolated resonator (resonant frequency, bandwidth, and efficiency) can serve as accurate predictors of antenna performance. The second step in the design process is to couple the resonator to a transmission line in such a way as to produce an impedance match at the resonant frequency. In Section IV, we considered the case of coupling the resonator to a coaxial transmission line. This case was chosen in order to maintain the axial symmetry in the geometry and enable the numerical simulation to be done in two dimensions. In general, the transmission line geometry that is chosen will depend upon the particular appl cation, and the design formalism described here applies to any chosen coupling geometry. The impedance matching problem can be understood by considering the antenna as a resonant coupler between two electromagnetic modes: the guided mode inside the transmission line, and the radiating TM_{10} spherical harmonic in free space. In any resonant coupling arrangement, there is a field coupling constant that characterizes the coupling of each of these modes to the resonator[37]. In order to produce an impedance match, the field coupling constants of the two modes to the resonator must be made equal (or equivalently, the rate at which energy flows into the resonator from one mode must equal the rate at which the resonator emits energy into the other mode). The coupling constant between the resonator and the free space mode is intrinsic to the resonator itself, and is directly related to the Q of the resonator. (The magnitude squared of this field coupling constant is known as the power factor[32], and is the inverse of the Q). The field coupling constant between the resonator and the transmission line mode is more difficult to determine, and depends upon the geometry of the resonator-transmission line coupling and the modal profiles of the resonator and transmission line modes. When designing the feed arrangement, it is important to pay attention to the modal profiles of these two modes, and to arrange the geometry such that there is sufficient coupling between the two modes to obtain an impedance match. As a general rule, we do not need to calculate the field coupling constant between the resonator and transmission line explicitly; rather, we can vary the geometry of the coupling and use numerical simulations to optimize the impedance match. This was the procedure followed in the previous section, where the stub/half-sphere geometry was chosen specifically because of the strong coupling it allowed between the transmission line and resonator mode; the length of the stub termination was then varied in order to tune the coupling and obtain the impedance match.

Based upon this formalism, we can expect that, for the antenna geometry of Figure 5, increasing the size of the resonator will increase its radiation power factor, and this will then require the length of the stub to be increased in order to preserve the impedance match (i.e., in order to provide a comparable increase in the coupling strength between the resonator and transmission line). Simulations conducted for a range of resonator sizes demonstrate this. Figure 8 plots the optimum stub length as a function of the radius of the hemispherical resonator. We see that larger resonators do require longer stub lengths in order to maintain a good impedance match. (The stub length values plotted are those for which the return loss was less than –30 dB at resonance.) As the radius increases above 10 mm, it appears that the optimum stub length will eventually become larger than the radius of the resonator (i.e., the solid line will cross the dashed line in the figure). Increasing the stub length beyond the radius of the resonator does not increase the coupling constant sufficiently to track the increasing radiation power factor of the resonator. For resonator sizes above 10.25 mm radius, it is not possible to achieve a good impedance match by simply increasing the length of the stub in this geometry. In order to design larger antennas based upon hemispherical resonators of this kind, changes in the coupling geometry will be required to increase the degree of coupling between the transmission line and the resonator.

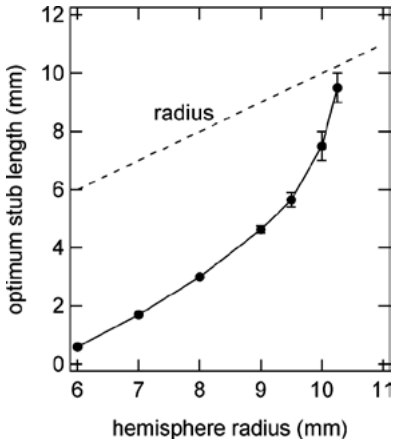

FIGURE 8

Optimum stub length of the antenna pictured in Figure 5 as a function of the radius of the negative permittivity sphere. The optimum stub length was determined by finding the length values that produced better than −30 dB return loss at resonance. The errors bars signify the ranges of length values that were deemed to be optimal. For radii above1 0.25 mm, the increasing stub length can no longer keep up with the increasing radiation power factor of the resonator (the length of the stub becomes longer than the radius of the sphere). In this regime, other changes in the coupling geometry will be required to produce effective antennas.

When absorption is present in the resonator material the total power factor of the resonator contains both radiation and absorption components. Thus, when absorption is added to the resonator material in an antenna design that was previously optimized under conditions of zero absorption, the coupling constant between the transmission line mode and the resonator must be increased (to compensate for the increase in the resonator power factor). We saw this in Section IV, when the stub length had to be increased from 3 to 4.5 mm after some absorption was added to the resonator material (Figure 7).

VI. PRACTICAL IMPLEMENTATION

This paper has examined the potential role of negative permittivity materials in improving the performance of electrically small antennas. Negative permittivity materials do not occur naturally at microwave frequencies, however, and they will have to be created in some form in order to realize antennas of the kind described in this paper. As discussed, negative permittivity can be realized at microwave frequencies using plasmas with an appropriate charge density. This is possible, for example, using gas discharge tubes[5–7]; however, a solid-state approach may be preferred for many applications. The carrier densities in metals produce plasma frequencies at ultraviolet wavelengths, while in doped semiconductors the plasma frequencies are typically found to be in the terahertz regime. It remains an open question as to whether an appropriate solid state material can be synthesized to produce plasma frequencies in the microwave regime.

The electromagnetic behavior associated with negative permittivity can be observed at microwave frequencies using the approach proposed by Pendry[9,38] and employed in recent studies of negative index metamaterials[13]. In a variation of this approach, Smith ***et al***.[39] employed a loop-wire medium to synthesize a negative permittivity response at microwave frequencies, and further constructed a crude spherical resonator based upon this approach, in which they experimentally observed a resonant response at a frequency below the plasma frequency of the composite medium. Their resonator was relatively large ($ka = 1.2$) compared to the structure discussed here, and the shape only roughly approximated that of a sphere. An alternative approach to achieving spherical resonators of this kind has recently been described by Stuart and Tran[40]. They demonstrated electrically small ($ka \backsim .05$) microwave resonators composed of arrays of non-interconnected printed circuit boards (PCBs) that achieve bandwidths at $\backsim 1.5\times$ the Chu limit. We believe an approach like that described in reference [40] offers a potential route towards achieving antennas of the sort described here. One appealing aspect of this approach to spherical antenna design is that a volumetric antenna can be constructed using purely planar building blocks that are not electrically connected with one another. In contrast to the two known spherical resonator designs discussed earlier (the spherical helix and spherical capped dipole), the resonator discussed in [40] is compatible with standard PCB manufacturing techniques. This sort of fabrication approach would likely be much simpler than for the aforementioned volumetric antennas when the operating frequency is high enough ($\backsim$multiple GHz) such that the physical size of the antenna becomes very small.

VII. SUMMARY

We have shown that resonators composed of negative permittivity materials can form the basis of effective small antenna elements. The resonant scattering properties of a sub-wavelength negative permittivity sphere are well described by a set of analytical formulas predicting its bandwidth and scattering efficiency. These formulas, derived from a quasi-static analysis, predict that the spherical resonator has a Q-factor that is only 1.5 times the Chu limit, making it an ideal candidate for use as an electrically small antenna. We have shown through finite element simulation how such an antenna can be constructed by coupling the resonator (a half-sphere above a ground plane) to a coaxial transmission line, forming an impedance matched radiating structure. The bandwidth and efficiency properties predicted by the quasi-static analysis of the isolated resonator correspond very well to the performance simulated in the antenna structure.

A comparison of the negative permittivity sphere to two known electrically small resonator designs (the folded spherical helix and the spherical capped dipole) shows that the bandwidth performance at 1.5 times the Chu limit is achieved in each resonator, a fact attributable to the spherical geometry common to all three. We believe this result is significant because it suggests that there are likely additional electrically small spherical resonator designs that can achieve this level of bandwidth performance: in particular, designs in which the inductance is spread more uniformly throughout the spherical volume, in a manner analogous to the negative permittivity sphere. Further, we believe our results will be of interest to the research community in the area of plasma antennas, as the ability of small spherical plasmas to closely approach Chu limit performance has not been widely appreciated. We hope that the results presented in this paper will stimulate interest in the study of a variety of sub-wavelength resonators and antennas based upon negative permittivity at the frequencies of interest.

VIII. REFERENCES

[1] H. A. Wheeler, "Fundamental limitations of small antennas," ***Proc. IRE***, vol. 35, pp. 1479–1484, 1947.

[2] L. J. Chu, "Physical limitations on omni-directional antennas," ***J. Appl. Phys.***, vol. 19, pp. 1163–1175, 1948.

[3] H. R. Raemer, "Radiation from linear electric or magnetic antennas surrounded by a spherical plasma shell," ***IRE Trans. Antennas Propag.,*** vol. 10, pp. 69–78, 1962.

[4] J. R. Wait, "Antennas in plasma," in ***Antenna Theory, Part 2,*** R. E. Collin and F. J. Zucker, Eds. New York: McGraw-Hill, 1969.

[5] K. M. Chen and C. C. Lin, "Enhanced radiation from a plasma-embedded antenna," ***Proc. IEEE***, vol. 56, pp. 1595–1597, 1968.

[6] G. G. Borg, J. H. Harris, D. G. Miljak, and N. M. Martin, "Application of plasma columns to radiofrequency antennas," ***Appl. Phys. Lett.,*** vol. 74, pp. 3272–3274, 1999.

[7] J. P. Rayner, A. P. Whichello, and A. D. Cheetham, "Physical characteristics of plasma antennas," ***IEEE Trans. Plasma Sci.,*** vol. 32, pp.269–281, 2004.

[8] W. Rotman, "Plasma simulation by artificial dielectrics and parallel-plate media," IRE Trans. Antennas Propag., vol. AP10, pp. 82–95, 1962.

[9] J. B. Pendry, A. J. Holden, W. J. Stewart, and I. Youngs, "Extremely low frequency plasmons in metallic mesostructures," ***Phys. Rev. Lett.,*** vol. 76, pp. 4773–4776, 1996.

[10] D. Sievenpiper, M. Sickmiller, and E. Yablonovitch, "3D wire mesh photonic crystals," ***Phys. Rev. Lett.,*** vol. 76, pp. 2480–2483, 1996.

[11] J. B. Pendry, A. J. Holden, D. J. Robbins, and W. J. Stewart, "Magnetism from conductors and enhanced nonlinear phenomena," ***IEEE Trans. Microw. Theory Tech.,*** vol. 47, pp. 2075–2084, 1999.

[12] D. R. Smith, W. J. Padilla, D. C. Vier, and S. C. Nemat Nasser, "Composite medium with simultaneously negative permeability and permittivity," ***Phys. Rev. Lett.,*** vol. 84, pp. 4184–4187, 2000.

[13] R. A. Shelby, D. R. Smith, and S. Schultz, "Experimental verification of a negative index of refraction," Science, vol. 292, pp. 77–79, 2001.

[14] A. A. Houck, J. B. Brock, and I. L. Chuang, "Experimental observations of a left-handed material that obeys Snell's law," ***Phys. Rev. Lett.,*** vol. 90, pp. 7401–7404, 2003.

[15] R. W. Ziolkowski and A. D. Kipple, "Application of double negative materials to increase the power radiated by electrically small antennas," ***IEEE Trans. Antennas Propag.***, vol. 51, pp. 2626–2640, 2003.

[16] N. Engheta and R. W. Ziolkowski, "A positive future for double-negative metamaterials," IEEE Trans. Microw. Theory Tech., vol. 53, pp. 1535–1556, 2005.

[17] R. W. Ziolkowski and A. D. Kipple, "Reciprocity between the effects of resonant scattering and enhanced radiated power by electrically small antennas in the presence of nested metamaterial shells," ***Phys. Rev. E***, vol. 72, p. 036602, 2005.

[18] C. F. Bohren and D. R. Huffman, ***Absorption and Scattering of Light by Small Particles.*** New York: Wiley, 1983.

[19] S. R. Best, "The radiation properties of electrically small folded spherical helix antennas," ***IEEE Trans. Antennas Propag.,*** vol. 52, pp. 953–960, 2004.

[20] ——, "Low Q electrically small linear and elliptical polarized spherical dipole antennas," ***IEEE Trans. Antennas Propag.,*** vol. 53, pp. 1047–1053, 2005.

[21] S. A. Tretyakov, S. I. Maslovski, A. A. Sochava, and C. R. Simovski,"The influence of complex material coverings on the quality factor of simple radiating systems," ***IEEE Trans. Antennas Propag.,*** vol. 53, pp. 965–970, 2005.

[22] H. A. Wheeler, "The spherical coil as an inductor, shield, or antenna," ***Proc. IRE,*** vol. 46, pp. 1595–1602, 1958.

[23] ***Electromagnetic Surface Modes,*** A. D. Boardman, Ed. New York: John Wiley & Sons, 1982.

[24] J. D. Jackson, ***Classical Electrodynamics,*** 2nd ed. New York: Wiley,1975.

[25] D. J. Griffiths, ***Introduction to Electrodynamics.*** Englewood Cliffs, NJ: Prentice Hall, 1989.

[26] J. D. Kraus, ***Antennas,*** 2nd ed. New York: McGraw-Hill, Inc., 1988.

[27] C. C. Chen, "Electromagnetic resonances of immersed dielectri spheres," ***IEEE Trans. Antennas Propag.,*** vol. 46, pp. 1074–1083, 1998.

[28] J. S. Mclean, "A re-examination of the fundamental limits on the radiation-Q of electrically small antennas," ***IEEE Trans. Antennas Propag.,*** vol. 44, pp. 672–676, 1996.

[29] A. Wokaun, J. P. Gordon, and P. F. Liao, "Radiation damping in surface-enhanced Raman scattering," ***Phys. Rev. Lett.,*** vol. 48, pp. 957–960, 1982.

[30] H. R. Stuart and D. G. Hall, "Island size effects in nanoparticle-enhanced photodetectors," ***Appl. Phys. Lett.,*** vol. 73, pp. 3815–3817, 1998.

[31] H. A. Wheeler, "The radiansphere around a small antenna," ***Proc. IRE,*** vol. 47, pp. 1325–1331, 1959.

[32] ——, "Small antennas," ***IEEE Trans. Antennas Propag.,*** vol. AP-23, pp. 462–469, 1975.

[33] N. Engheta, A. Salandrino, and A. Alu, "Circuit elements at optical frequencies: nanoinductors, nanocapacitors, and nanoresistors," ***Phys. Rev. Lett.,*** vol. 95, p. 095504, 2005.

[34] H. D. Foltz, J. S. McLean, and G. Crook, "Disk-loaded monopoles with parallel strip elements," ***IEEE Trans. Antennas Propag.,*** vol. 46, pp. 1894–1896, 1998.

[35] FEMLAB Ver. 3.1 COMSOL, Inc., 2004.

[36] A. D. Yaghjian and S. R. Best, "Impedance, bandwidth, and Q of antennas," ***IEEE Trans. Antennas Propag.,*** vol. 53, p. 1298, 2005.

[37] A. Yariv, "Universal relations for coupling of optical power between microresonators and dielectric waveguides," ***Elec. Lett.,*** vol. 36, pp. 321–322, 2000.

[38] S. I. Maslovski, S. A. Tretyakov, and P. A. Belov, "Wire media with negative effective permittivity: a quasi-static model," ***Microw. Opt. Technol. Lett.,*** vol. 35, p. 47, 2002.

[39] D. R. Smith, D. C. Vier, W. Padilla, and S. C. Nemat Nasser, "Loop-wire medium for investigating plasmons at microwave frequencies," ***Appl. Phys. Lett.,*** vol. 75, p. 1425, 1999.

[40] H. R. Stuart and C. Tran, "Subwavelength microwave resonators exhibiting strong coupling to radiation modes," ***Appl. Phys. Lett.,*** vol. 87, p. 151108, 2005.

Howard R. Stuart (M'98) received the S.B. and S.M. degrees in electrical engineering from the Massachusetts Institute of Technology, Cambridge, in 1988 and 1990, respectively, and the Ph.D. degree in optics from the University of Rochester, Rochester, NY, in 1998. From 1990 to 1993, he worked as a Research Scientist for the Polaroid Corporation in Cambridge, MA. In 1998, he became a Member of Technical Staff at Bell Laboratories, Lucent Technologies, Holmdel, NJ, from which he transferred to the Whippany, NJ, location in 2003. He has published papers in the areas of metal nanoparticle enhanced photodetection, multimode fiber transmission, optical waveguide interactions and devices, optical MEMS, optical performance monitoring, and electrically small microwave resonators and antennas. He has served as the Integrated Optics Topical Editor for the ***OSA*** journal ***Applied Optics*** since 2002.

Alex Pidwerbetsky (M'84) received the B.S. degree in physics from Rensselaer Polytechnic Institute, Troy, NY, and the M.S. and Ph.D. degrees in applied physics from Cornell University, Ithaca, NY. His graduate dissertation was on simulation and analysis of wave propagation through random media. He is a Consulting Member of Technical Staff in Bell Laboratories, Lucent Technologies, Whippany, NJ. He is involved in a number of research programs in radio and optical wireless communications science and technology. He is currently the Principal Investigator for DARPA's Mobile Network Multiple Input Multiple Output (MIMO) program. He is also a key member of Bell Labs' Coherent Communications Imaging and Targeting program. Previously, he was the Principal Investigator for the effort to achieve very high spectral efficiencies in outdoor environments using BLAST MIMO technology under DARPA's Next Generation Internet program as well as the Principal Investigator for a DARPA effort to apply BLAST to FCS-Communications. Additionally, he was the Principal Investigator for an ARPA effort integrating the low-cost wireless infrastructure enabled by the RF tag technology with sensors on a chip, creating a new generation of wireless distributed sensor networks. He has also conducted concept definition, studies, and analyses in support of DARPA's Small Unit Operations program with respect to wireless communications. He has extensive experience in modeling, data analysis, system analysis, simulation, and concept development. He has served as Chief Scientist and Deputy Test Director for the DARPA/AT&T Decision Support System and DARPA/AT&T Acoustic Warfare Simulator. He is the co-inventor for five issued and four pending U.S. patent applications in the area of wireless communications. While at Cornell University, he was with the Center for Radiophysics and Space Research. Previous to that he was a Researcher at General Electric's Corporate Research and Development Center.